

# Paradox resolved: stop signal race model with negative dependence

Hans Colonius<sup>a,c,1</sup> and Adele Diederich<sup>b,1,2</sup>

<sup>a</sup>Oldenburg University; <sup>b</sup>Jacobs University Bremen

This manuscript was compiled on February 18, 2018

**The ability to inhibit our responses voluntarily is an important case of cognitive control. The stop-signal paradigm is a popular tool to study response inhibition. Participants perform a response time task (*go task*) and, occasionally, the go stimulus is followed by a stop signal after a variable delay, indicating subjects to withhold their response (*stop task*). The main interest of modeling is in estimating the unobservable stop-signal processing time, that is, the covert latency of the stopping process as a characterization of the response inhibition mechanism. In the *independent race model* the stop-signal task is represented as a race between stochastically independent go and stop processes. Without making any specific distributional assumptions about the processing times, the model allows to estimate the mean time to cancel a response. However, neurophysiological studies on countermanding saccadic eye movements have shown that neural correlates of go and stop processes consist of networks of mutually *interacting* gaze-shifting and gaze-holding neurons. This poses a major challenge in formulating linking propositions between the behavioral and neural findings. Here we propose a *dependent race model* that postulates perfect negative stochastic dependence between go and stop activations. The model is consistent with the concept of interacting processes while retaining the simplicity and elegance of the distribution-free independent race model. For mean data, the dependent model's predictions remain identical to those of the independent model. The resolution of this apparent paradox advances the understanding of mechanisms of response inhibition and paves the way for modeling more complex situations.**

response inhibition | stop signal paradigm | independent race model | perfect negative dependence

A recurrent theme in cognitive modeling is the difficulty to uniquely identify the processes underlying the generation of response times and probabilities in behavioral paradigms like simple yes-no tasks or same-different judgments of stimulus pairs. A prime example is the serial vs. parallel processing issue (1–3) showing that even rigorous mathematical analyses of the underlying assumptions may not always resolve the difficulty completely. Recently, efforts in model-based cognitive neuroscience to constrain behavioral models by findings obtained from neuroscientific methods have intensified, from spike train analyses to EEG and fMRI recordings (4). One area where important advances have emerged from this joint endeavor is the modeling of cognitive control and, in particular, response inhibition (5, 6). Response inhibition refers to the ability to suppress responses that are no longer required or have become inappropriate; it is important for survival, such as stopping yourself from crossing the street when a car comes around the corner without noticing you. Deficits of response inhibition have been linked to several disorders like attention-deficit/hyperactivity, obsessive-compulsive behavior and substance abuse. Probing response inhibition has been used widely to study executive control and flexibility in behavior; for reviews, see (6–9) and a recent theme issue of *Philosophical Transactions of the Royal Society B* (2017) on ‘Movement suppression: brain mechanisms for stopping and stillness’ (10)

In the laboratory, a very useful tool for the study of inhibition is the *stop-signal paradigm* where participants perform a response time task (*go task*), such as moving their gaze to the location of a pre-defined target. Occasionally, the go stimulus is followed by a stop signal after a variable time delay, indicating subjects to withhold the response (*stop task*). Performance in the stop-signal paradigm has been modeled as a race between a “go process”, triggered by the presentation of the go stimulus, and a “stop process” triggered by the presentation of the stop signal (6, 8). When the stop process finishes before the go process, the response is inhibited; otherwise, it is executed. The main interest of the modeler is in estimating the unobservable stop-signal reaction time (SSRT), that is, the latency of the stopping process as a characterization of the response inhibition mechanism. In the *independent race model* (IND model, for short) the stop-signal task is represented as a race between *stochastically independent* go and stop processes (11). Under certain simplifying assumptions, mean SSRT can be estimated efficiently without making any specific assumptions about the distribution of the processing times (6). In several hundreds of studies, the IND model has been applied in virtually every stop-signal experiment providing important measures of cognitive control like SSRT. Although the model makes no commitment to the underlying computational or neural processes that generate the go and stop processing times, the IND model is considered as defining constraints that any model of response inhibition must follow (12).

However, neurophysiological studies in the frontal eye fields (FEF) and superior colliculus (SC) of macaque monkeys performing a countermanding task with saccadic eye movements have shown that the neural correlates of go and stop processes produce eye movement behavior through a network of *interacting* gaze-shifting and gaze-holding neurons (13–16). This discrepancy between the behavioral and neural data is widely perceived as a paradox (9, 12, 17, 18): how can interacting circuits of mutually inhibitory neurons instantiate stop and go processes with stochastically independent finishing times?

Here we propose a variant of the race model which, instead of independence, assumes *perfect negative stochastic dependence* between go and stop processes (PND model, for short). It resolves the apparent paradox and nonetheless retains the distribution-free property of the independent race model. Moreover, the PND model's predictions, considered at the level of mean SSRT, are shown to be necessarily identical to those of the independent model. Notably, we argue that it is very difficult to empirically

125 distinguish between the two race model versions without introducing further, parametric assumptions. Thus, there is no reason 187  
126 to uphold the stochastic independence assumption of the race model whenever a distribution-free version is to be considered. 188

127  
128 **Neurally inspired modeling** 190

129 Investigating the neural underpinnings of response inhibition in saccades, Hanes and Schall (13) first showed that macaque 191  
130 monkey behavior in saccade countermanding corresponded in detail to that of human performance in manual stop-signal tasks. 192  
131 Then, recording from the frontal eye fields they isolated neurons involved in gaze-shifting and gaze-holding that represent 193  
132 a larger circuit of such neurons that extends from cortex through basal ganglia and superior colliculus to brainstem (14). 194  
133 Importantly, that result was based on their postulate that for neurons to participate in controlling movement initiation two 195  
134 criteria must be met: first, neurons must discharge differently when movements are initiated or withheld; if neurons still 196  
135 discharge when movements are canceled, their activity was not affected by the stop process. Second, the differential modulation 197  
136 on canceled trials must occur before SSRT; otherwise, the neural modulation happens after the movement has already been 198  
137 canceled (18, p.1012). From these findings, Boucher and colleagues (17) developed an *interactive race model* linking the 199  
138 interacting circuits of mutually inhibitory gaze-holding and gaze-shifting neurons with stochastic accumulation in the go and 200  
139 stop processes of the race model (see also 19). A response is observed only if the go process reaches a certain threshold of 201  
140 activation. Stopping occurs if the stop process interferes with the go process by inhibiting activation in the go accumulator to 202  
141 prevent it from reaching the threshold. Alternative models assume that response inhibition results from blocking the input to 203  
142 the go unit (“blocked-input models”) (20) or postulate a spiking neural network of hundreds of units representing populations 204  
143 of movement neurons, fixation neurons and inhibitory interneurons, and a control unit that turns the fixation neurons on and 205  
144 off (21). 206

145 These neural models are computationally explicit: they are based on systems of stochastic differential equations; estimating 207  
146 parameters to best fit the behavioral data, they are able to predict the distribution of cancel times, i.e., the times at which 208  
147 neural activity modulates on trials on which subjects stop successfully, relative to SSRT (12). The models fit the behavioral 209  
148 data just as well as the independent race model. Note that this is just another instantiation of the paradox. An attempt to 210  
149 resolve the contradiction between stochastic independence for behavioral data and interdependence at the neural level has been 211  
150 to postulate that the stop process is independent of the go process for much of its duration, followed by a late and potent 212  
151 interaction between stopping and going that reverses the trajectory of go activation (12, 17). Strictly speaking, this would 213  
152 require introducing two subsequent processing stages in the IND model, independence followed by strong interaction. No 214  
153 formal modeling of this extension has been undertaken, however, to the best of our knowledge. 215

154  
155 **Background: General race model** 217

156  
157 Next, we present a formal framework for the general race model making no assumption at all about the dependency between 219  
158 stop and go processes. One should distinguish between two different experimental conditions termed context  $\mathcal{GO}$  where only a 220  
159 go signal is presented, and context  $\mathcal{STOP}$  where a stop signal is presented in addition. A race between processes triggered by 221  
160 the go and stop signal is represented by two random variables:  $T_{go}$  and  $T_{stop}$  (referred to as SSRT above) denote the random 222  
161 processing times for the go and stop signal, respectively, in context  $\mathcal{STOP}$  with a bivariate distribution function denoted  $H$ , 223

$$162 \quad H(s, t) = \Pr[T_{go} \leq s, T_{stop} \leq t], \quad [1] \quad 224$$

163 defined for all real numbers  $s$  and  $t$ , with  $s, t \geq 0$ . The marginal distributions of  $H(s, t)$  are 225

$$164 \quad F_{go}(s) = \Pr[T_{go} \leq s, T_{stop} < \infty] \text{ and} \quad 226$$

$$165 \quad F_{stop}(t) = \Pr[T_{go} < \infty, T_{stop} \leq t]. \quad 227$$

166  
167 In context  $\mathcal{STOP}$  the go signal triggers a realization of random variable  $T_{go}$  and the stop signal triggers a realization of random 230  
168 variable  $T_{stop}$ . In context  $\mathcal{GO}$ , however, only processing of the go signal occurs. In general, the latter one may be different from 231  
169 the marginal distribution  $F_{go}(s)$  in context  $\mathcal{STOP}$ . However, the *general race model* rules this out by adding the important 232  
170 assumption of “context invariance”, also know as “context independence” (e.g. 9): 233

171  
172  
173

### 174 Significance Statement 236

175  
176 The ability to suppress a response that is no longer required or has become inappropriate is an important act of cognitive control. 238  
177 Deficits in inhibiting a response to a stop signal have been linked to disorders like attention-deficit/hyperactivity. A widely accepted 239  
178 model for the stop signal paradigm assumes that stop signal processing occurs independently from go signal processing and permits 240  
179 to estimate the covert latency of the stop process. However, neurophysiological data suggest interactive neural networks of going 241  
180 and stopping raising a contradiction between the behavioral and neural findings. Introducing a model with strong negative stochastic 242  
181 dependency between go and stop processing resolves the paradox while retaining the computational simplicity of the original model. 243

182  
183

184 Authors declare no conflict of interest. 245

185 <sup>1</sup>H.C. and A.D. contributed equally to this work. 246

186 <sup>2</sup>To whom correspondence should be addressed. E-mail: hans.colonius@uni-oldenburg.de 247

249 **Context invariance (CI).** In context  $\mathcal{GO}$ , the distribution of go signal processing time is assumed to be 311  
 250 
$$F_{go}(s) = \Pr[T_{go} \leq s, T_{stop} < \infty],$$
 312 [2] 313  
 251  
 252 i.e., it is identical to the marginal distribution  $F_{go}(s)$  in context  $\mathcal{STOP}$ . 314  
 253 From these assumptions, the probability of observing a response to the go signal, given a stop signal is presented with delay 315  
 254  $t_d$  [ms] ( $t_d \geq 0$ ) after the go signal, is defined by 316  
 255 
$$p_r(t_d) = \Pr[T_{go} < T_{stop} + t_d].$$
 317 [3] 318  
 256 According to the model, the probability of observing a response to the go signal no later than time  $t$ , given the stop signal was 319  
 257 presented with delay  $t_d$ , is given by (conditional) distribution function 320  
 258 
$$F_{sr}(t | t_d) = \Pr[T_{go} \leq t | T_{go} < T_{stop} + t_d],$$
 321 [4] 322  
 259 known as *signal-response RT* distribution. 323  
 260 The main interest in race modeling is to obtain information about the distribution of the unobservable stop signal processing 324  
 261 time  $T_{stop}$ , or about some of its parameters, given sample estimates of  $F_{go}(t)$ ,  $F_{sr}(t | t_d)$ , and  $p_r(t_d)$ . As observed in (11), 325  
 262 letting stop signal delay  $t_d$  vary, the *inhibition function*  $p_r(t_d)$  can be formally considered as the distribution function of a 326  
 263 random variable,  $T_d \equiv T_{go} - T_{stop}$ , say. Then, 327  
 264 
$$E[T_d] = E[T_{go}] - E[T_{stop}],$$
 328 [5] 329  
 265 with  $E[\cdot]$  denoting expected value (mean) of a random variable. Solving for the estimate of  $E[T_{stop}]$  immediately yields an 330  
 266 estimate of the mean of the unobservable distribution of  $T_{stop}$ . It is well known that the reliability of this estimation method, 331  
 267 known as the *mean method*, depends on how precise the inhibition function  $p_r(t_d)$  and the mean of  $T_{go}$  are estimated (6, 9). 332  
 268 Obtaining estimates of higher moments, or the entire distribution of  $T_{stop}$ , requires further non-parametric assumptions about 333  
 269 the bivariate distribution  $H(s, t)$ . 334  
 270  
 271 **Independent vs. negatively dependent race model** 335  
 272  
 273 The most common version of the race model, as introduced by Logan & Cowan (11), postulates stochastic independence 336  
 274 between  $T_{go}$  and  $T_{stop}$ : 337  
 275 **Stochastic independence:** 338  
 276 
$$H(s, t) = \Pr[T_{go} \leq s] \times \Pr[T_{stop} \leq t] = F_{go}(s) \times F_{stop}(t),$$
 339  
 277 for all  $s, t$  ( $s, t \geq 0$ ). 340  
 278 In addition to estimating the mean via Equation [5], an estimate of the variance of stop signal processing time is obtainable 341  
 279 in the IND model from 342  
 280 
$$\text{Var}[T_{stop}] = \text{Var}[T_d] - \text{Var}[T_{go}],$$
 343 [6] 344  
 281 due to assuming stochastic independence. Finally, it can be shown that the unobservable stop signal distribution function 345  
 282  $F_{stop}(t)$  is expressible as a function of the observables  $p_r(t_d)$ ,  $f_{go}(t)$  and  $F_{sr}(t | t_d)$  (see Methods section). 346  
 283 In order to resolve the paradox described above, a race model with negative dependency between go and stop signal 347  
 284 processing times is proposed next. We define a bivariate distribution function for  $T_{go}$  and  $T_{stop}$  exhibiting *perfect negative* 348  
 285 *dependence* (see, e.g., 22) as follows : 349  
 286 **Perfect negative stochastic dependence:** 350  
 287 
$$H^-(s, t) = \max\{F_{go}(s) + F_{stop}(t) - 1, 0\}.$$
 351 [7] 352  
 288 for all  $s, t$  ( $s, t \geq 0$ ). The marginal distributions of  $H^-(s, t)$  are the same as before, that is,  $F_{go}(s)$  and  $F_{stop}(t)$ . Note that this 353  
 289 perfect negative stochastic dependence (PND) model is parameter-free just like the IND race model, that is, we do not assume 354  
 290 some specific parametric distribution. It can be shown (see Methods) that then 355  
 291 
$$F_{stop}(T_{stop}) = 1 - F_{go}(T_{go})$$
 356 [8] 357  
 292 holds “almost surely”, that is, with probability 1. Thus, for any  $F_{go}$  percentile we immediately obtain the corresponding  $F_{stop}$  358  
 293 percentile as complementary probability and vice versa, expressing perfect negative dependence between  $T_{go}$  and  $T_{stop}$ . The 359  
 294 relation in Equation [8] is also interpretable as “ $T_{stop}$  is (almost surely) a decreasing function of  $T_{go}$ ”. 360  
 295 The PND model arguably constitutes the most direct implementation of the notion of “mutual inhibition” observed in 361  
 296 neural data: any increase of inhibitory activity (speed-up of  $T_{stop}$ ) elicits a corresponding decrease in “go” activity (slow-down 362  
 297 of  $T_{go}$ ) and vice versa. 363  
 298 **Predictions from the PND race model.** We list some predictions from the PND race model (for further details, see Methods 364  
 299 section): 365  
 300 **Probability of stopping.** Under perfect negative dependence between  $T_{go}$  and  $T_{stop}$ , the probability of stopping  $p_r(t_d)$  is an 366  
 301 increasing function of  $t_d$ , as it should. 367  
 302  
 303  
 304  
 305  
 306  
 307  
 308  
 309  
 310

373 **Signal-response RT distribution.** Signal-response RT distribution 435  
374 436  
375  $F_{sr}(t|t_d) = \Pr[T_{go} \leq t | T_{go} < T_{stop} + t_d],$  [4] 437  
376 438  
377 approaches the go signal distribution  $F_{go}(t)$  with increasing stop signal delay  $t_d$ . Moreover, for varying values of  $t_d$ ,  $F_{sr}(t|t_d)$  439  
378 exhibits the “fan effect” typically found in empirical data and also predicted by the IND race model (6, 11). 440  
379 To illustrate, Figure 1 presents the go signal distribution and signal-response RT distributions with different delay values  $t_d$  441  
380 for both the IND (dashed curves) and the PND race model (solid lines) assuming exponential distributions for  $T_{go}$  and  $T_{stop}$ . 442  
381 While the exponential distribution lacks empirical support, it was chosen here just to illustrate quantitative differences between 443  
382 the model versions. 444  
383 An important feature of the PND model is suggested by Figure 1: each signal-response distribution  $F_{sr}(t|t_d)$  crosses 1 at 445  
384 a certain finite point  $t$ . It is shown below that this point is predictable from the observables  $p_r(t_d)$  and  $F_{go}(t)$ . While this 446  
385 “crossing” property is not shared by the IND model (because the “coupling” of  $T_{go}$  and  $T_{stop}$  as expressed in Equation (8) is 447  
386 absent), the strength of this test will of course depend on the precision of estimates of  $F_{sr}(t|t_d)$ . 448  
387 **Estimating moments of the  $T_{stop}$  distribution.** Given that the marginal distributions  $F_{go}$  and  $F_{stop}$  are the same under both 449  
388 models, any estimates for  $E[T_{stop}]$  based on the mean method (Eq. [5]) are necessarily identical for the IND and PND model. 450  
389 However, for the variance we obtain 451  
390 452  
391 
$$\text{Var}[T_{stop}] = \text{Var}[T_d] - \text{Var}[T_{go}] + 2 \text{Cov}[T_{go}, T_{stop}].$$
 [9] 453  
392 454  
393 As the covariance in the above equation is unknown, an estimate for the stop signal variance is no longer available under the 455  
394 PND model. Nevertheless, given that  $\text{Cov}[T_{go}, T_{stop}]$  is the most extreme negative covariance under any bivariate distribution 456  
395 for  $T_{go}$  and  $T_{stop}$  (23), the PND model stop signal variance can never be larger than the one under independence. 457  
396 458  
397 **Discussion** 459  
398 460  
399 **Testing IND vs. PND race models.** Because stop signal processing times are not observable, empirical testing of non-parametric 461  
400 stop signal race models is severely limited in general. In particular, both the IND and PND version of the race model can only 462  
401 be tested in conjunction with context invariance (CI). Presuming CI is valid, the following predictions can be tested: (1) mean 463  
402 signal-response RT should be faster than mean go signal RT; (2) mean signal-response RT should increase with stop signal 464  
403 delay  $t_d$ ; and (3) both these tests are implied by the “fan” structure of the distribution functions permitting an additional 465  
404 qualitative test of IND and PND race models. Because data not consistent with this “fan” structure would be evidence against 466  
405 both the IND and PND model, obviously, none of these tests would allow us to distinguish between IND and PND. 467  
406 By construction, the PND model has the same distribution for stop signal processing as the IND model; therefore, estimates 468  
407 for mean SSRT, i.e., the expected value of stop signal processing, will be identical for either model as long as estimates are 469  
408 based on the mean method. In a sense, this is good news because it implies that adopting perfect negative dependency between 470  
409 go and stop signal processing does not invalidate previous SSRT estimates of all empirical studies employing the mean method. 471  
410 Note that this holds as well for estimating SSRT via the *integration method*, another way to estimate SSRT. However, because 472  
411 the integration method presumes stop signal processing time to be constant, the distinction between IND and PND model 473  
412 becomes meaningless. 474  
413 This leaves us with the shape of the family of signal-response distributions, that is,  $F_{sr}(t|t_d)$  for varying values of  $t_d$ , as the 475  
414 only potential means of distinguishing between the two models. Whether or not this “crossing” test that -as outlined above- 476  
415 consists of checking the way in which the signal-response distributions approach their upper bound of 1, proves to be as visible 477  
416 in real data compared to the exponential toy example (Figure 1) will depend on the specific, but unobservable, stop signal 478  
417 distribution. 479  
418 480  
419 **Conclusion.** Several authors have stressed that the level of description provided by the race model is quite different from that 481  
420 of neural models (17, 20): the independent race model is mute about the possible underlying mechanisms of response inhibition, 482  
421 and its primary purpose is to provide a measure of stop signal processing time, which the model allows without having to 483  
422 assume a specific distribution or estimate parameters. Nevertheless, it has been claimed that the independent race model 484  
423 “captures the essence of computation and ...that it formulates the constraints that any model of response inhibition must follow” 485  
424 (cf. 20, p.3). The race model with perfect negative dependence suggested here operates at the same level of generality and 486  
425 yields the same measure of (mean) stop signal processing time but, importantly, resolves the paradox the independent model is 487  
426 facing due to the neurophysiological findings. We conclude that the race model with perfect negative stochastic dependence is 488  
427 a natural way to unify the observation of interacting circuits of mutually inhibitory gaze-holding and gaze-shifting neurons 489  
428 with data on the behavioral level. 490  
429 Beyond the simple stop signal task, several other forms of acts of control have been studied that pose an even greater 491  
430 challenge for efforts to identify the underlying cognitive processes, such as switching tasks or shifting of attention (5). One 492  
431 promising area is *selective stopping* where response inhibition is required for some stimuli (e.g. red light) but not others (green 493  
432 light) (e.g., 24). Representing cognitive processes for such more complex tasks may call for types of graded, instead of perfect, 494  
433 dependency. Appropriate race models can easily be introduced by appealing to more general forms of stochastic dependency 495  
434 via copulas (22). 496

497 **Methods** 559

498 This section presents some computational details for both the IND and PND model, in general and for the special case of 560  
 499 exponential distributions (for producing Figure 1). 561

500 We assume that distribution functions  $F_{go}$  and  $F_{stop}$  possess densities,  $f_{go}$  and  $f_{stop}$ , and are increasing, where “increasing” 562  
 501 always refers to “strictly increasing” here. Note that although it is usually taken for granted in the race model that densities 563  
 502 exist, strictly speaking, this is not required neither by the independent nor the dependent race model. 564  
 503 565

504 **Independent race model.** Under stochastic independence of  $T_{go}$  and  $T_{stop}$ , 566

$$\begin{aligned}
 p_r(t_d) &= \Pr[T_{go} < T_{stop} + t_d] \\
 &= \int_0^\infty f_{go}(t)[1 - F_{stop}(t - t_d)] dt.
 \end{aligned}
 \tag{10}$$

509 Moreover, 571

$$\text{Var}[T_d] = \text{Var}[T_{stop}] + \text{Var}[T_{go}],
 \tag{11}$$

511 implying Equation [6]. 572

512 Writing  $f_{sr}(t | t_d)$  for the density function of signal-response time distribution  $F_{sr}(t | t_d)$ , it has been shown in (25) that 573  
 513 574

$$f_{sr}(t | t_d) = f_{go}(t) [1 - F_{stop}(t - t_d)] / p_r(t_d).
 \tag{12}$$

514 From that, an explicit expression of the distribution of the unobservable stop signal processing time  $T_{stop}$  is given by: 575  
 515 576  
 516 577

$$F_{stop}(t - t_d) = 1 - \frac{f_{sr}(t | t_d)p_r(t_d)}{f_{go}(t)}.
 \tag{13}$$

517 579  
 518 580  
 519 Unfortunately, as investigated in (26, 27), gaining reliable estimates for the stop signal distribution using Equation [13] requires 581  
 520 unrealistically large numbers of observations. 582  
 521 583

522 **Perfect negative dependent race model.** Defining the bivariate distribution by 584

$$H^-(s, t) = \max\{F_{go}(s) + F_{stop}(t) - 1, 0\}
 \tag{7}$$

523 for all  $s, t$  ( $s, t \geq 0$ ), the marginal distributions of  $H^-(s, t)$  are again  $F_{go}(s)$  and  $F_{stop}(t)$ . A classic result from the *theory of* 585  
 524 *copulas* (see SI) asserts that 586  
 525 587

526 (i)  $H^-$  is the lower bound of all bivariate distributions  $H$  of  $(T_{go}, T_{stop})$ , i.e.,  $H^-(s, t) \leq H(s, t)$  for all  $(s, t)$ ; 588  
 527 589

528 (ii)  $\Pr[F_{go}(T_{go}) + F_{stop}(T_{stop}) = 1] = 1$ . 590  
 529 591

530 From (i) the covariance between the random variables can be shown to be the smallest possible across all bivariate distributions 592  
 531  $H(s, t)$  (23). Statement (ii) is equivalent to 593

$$F_{stop}(T_{stop}) = 1 - F_{go}(T_{go}).
 \tag{8}$$

532 holding almost surely. 594  
 533 595

534 **Probability of stopping.** Under perfect negative dependence between  $T_{go}$  and  $T_{stop}$ , 596  
 535 597

$$\begin{aligned}
 p_r(t_d) &= \Pr[T_{go} - T_{stop} < t_d] \\
 &= \Pr[T_{go} - F_{stop}^{-1}[1 - F_{go}(T_{go})] < t_d] \\
 &= \Pr[g(T_{go}) < t_d] \\
 &= \Pr[T_{go} < g^{-1}(t_d)],
 \end{aligned}
 \tag{14}$$

536 598  
 537 599  
 538 600  
 539 601  
 540 602  
 541 603  
 542 where function  $g$ , defined as  $g(t) = t - F_{stop}^{-1}[1 - F_{go}(t)]$ , is increasing and so its inverse  $g^{-1}$  is increasing as well. Thus,  $p_r(t_d)$  604  
 543 is increasing in  $t_d$ . 605  
 544 606

545 **Signal-response RT distribution.** For stop signal delay  $t_d$ , 607

$$\begin{aligned}
 F_{sr}(t | t_d) &= \Pr[T_{go} \leq t | T_{go} < T_{stop} + t_d] \\
 &= \Pr[T_{go} \leq t \cap T_{go} < T_{stop} + t_d] / p_r(t_d) \\
 &= \Pr[T_{go} \leq t \cap T_{go} < g^{-1}(t_d)] / \Pr[T_{go} < g^{-1}(t_d)] \\
 &= F_{go}(\min\{t, g^{-1}(t_d)\}) / F_{go}(g^{-1}(t_d)).
 \end{aligned}$$

546 608  
 547 609  
 548 610  
 549 611  
 550 612  
 551 To see that  $F_{sr}(t | t_d)$  obeys the “fan effect” consider two different delays,  $t_d$  and  $t_d^*$ , say, with  $t_d < t_d^*$ ; for a fixed value of  $t$ , we 613  
 552 first assume  $t < g^{-1}(t_d) < g^{-1}(t_d^*)$ . Then 614  
 553 615

$$\begin{aligned}
 F_{sr}(t | t_d^*) &= F_{go}(t) / F_{go}(g^{-1}(t_d^*)) \\
 &< F_{go}(t) / F_{go}(g^{-1}(t_d)) \\
 &= F_{sr}(t | t_d).
 \end{aligned}$$

554 616  
 555 617  
 556 618  
 557 619  
 558 The cases  $g^{-1}(t_d) < t < g^{-1}(t_d^*)$  and  $g^{-1}(t_d) < g^{-1}(t_d^*) < t$  can be shown similarly. 620

621 **Expected stop signal processing time.** A formal expression for mean (expected) stop signal processing time is obtained as follows. 683  
 622 We have 684

$$\begin{aligned} E[T_{stop}] &= \int_0^\infty [1 - F_{stop}(s)] ds & 685 \\ &= \int_\infty^0 F_{go}(t) \frac{ds}{dt} dt \quad (\text{a.s.}), & 686 \end{aligned} \tag{15}$$

626 687  
 627 688  
 628 689  
 629 using Equation [8] and the fact that  $1 - F_{stop}(s)$  and  $F_{go}(t)$  have opposite limit values. With 691  
 630 692

$$s = F_{stop}^{-1}[1 - F_{go}(t)] \tag{15}$$

631 693  
 632 694  
 633 we have 695

$$\frac{ds}{dt} = -f_{go}(t)/f_{stop} [F_{stop}^{-1}[1 - F_{go}(t)]] . \tag{15}$$

634 696  
 635 697  
 636 698  
 637 Inserting into [15] yields 699

$$E[T_{stop}] = \int_0^\infty \frac{F_{go}(t) f_{go}(t)}{f_{stop} [F_{stop}^{-1}[1 - F_{go}(t)]]} dt. \tag{16}$$

638 700  
 639 701  
 640 702  
 641 **IND model: exponential case.** Define independent, exponential distributions for  $T_{go}$  and  $T_{stop}$  with parameters  $\lambda_{go} > 0$  and 703  
 642  $\lambda_{stop} > 0$  for context *STOP* by 704

$$\begin{aligned} H(s, t) &= \Pr[T_{go} \leq s] \times \Pr[T_{stop} \leq t] & 705 \\ &= (1 - \exp[-\lambda_{go} s]) \times (1 - \exp[-\lambda_{stop} t]), & 706 \end{aligned}$$

643 707  
 644 708  
 645 709  
 646 710  
 647 for all  $s, t \geq 0$ . Then 711

$$\begin{aligned} p_r(t_d) &= \int_0^{t_d} f_{go}(t) dt + \int_{t_d}^\infty f_{go}(t) [1 - F_{stop}(t - t_d)] dt & 712 \\ &= 1 - \frac{\lambda_{stop}}{\lambda_{stop} + \lambda_{go}} \exp[-\lambda_{go} t_d]. & 713 \end{aligned} \tag{17}$$

648 714  
 649 715  
 650 716  
 651 717  
 652 718  
 653 719  
 654 720  
 655 For  $t > t_d$ , the density of the signal-response distribution is given by, 721

$$\begin{aligned} f_{sr}(t | t_d) &= f_{go}(t) [1 - F_{stop}(t - t_d)] / p_r(t_d) & 722 \\ &= \frac{\lambda_{go} \exp[-\lambda_{go} t] \exp[-\lambda_{stop}(t - t_d)]}{\left(1 - \frac{\lambda_{stop}}{\lambda_{stop} + \lambda_{go}} \exp[-\lambda_{go} t_d]\right)} & 723 \\ &= \frac{1}{K} (\lambda_{go} + \lambda_{stop}) \exp[-(\lambda_{go} + \lambda_{stop})(t - t_d)], & 724 \end{aligned} \tag{18}$$

656 725  
 657 726  
 658 727  
 659 728  
 660 729  
 661 730  
 662 731  
 663 732  
 664 with  $K = \exp[\lambda_{go} t_d] (1 + \lambda_{stop}/\lambda_{go}) - \lambda_{stop}/\lambda_{go}$ . For  $t_d = 0$ , we have  $K = 1$  and the signal-response density is identical to an 733  
 665 exponential density for an independent race between  $T_{stop}$  and  $T_{go}$ , with parameter  $\lambda_{go} + \lambda_{stop}$  and  $p_r(t_d) = \lambda_{go}/(\lambda_{go} + \lambda_{stop})$ . 734  
 666 For  $t \leq t_d$ , the density simplifies to 735

$$\begin{aligned} f_{sr}(t | t_d) &= f_{go}(t) / p_r(t_d) & 736 \\ &= \frac{1}{\lambda_{stop} + \lambda_{go}} \exp[-\lambda_{go}(t - t_d)]. & 737 \end{aligned} \tag{19}$$

667 738  
 668 739  
 669 740  
 670 741  
 671 742  
 672 Computation of the expected value of signal-response RTs yields: 743  
 673 744

$$\begin{aligned} E[T_{go} | T_{go} < T_{stop} + t_d] &= \int_0^\infty t f_{sr}(t | t_d) dt & 745 \\ &= \frac{\lambda_{go} [1 + (\lambda_{go} + \lambda_{stop}) t_d]}{(\lambda_{go} + \lambda_{stop}) \{ \exp[\lambda_{go} t_d] (\lambda_{go} + \lambda_{stop}) - \lambda_{stop} \}}. & 746 \end{aligned} \tag{20}$$

674 747  
 675 748  
 676 749  
 677 750  
 678 751  
 679 752  
 680 753  
 681 In particular, for  $t_d = 0$ , we obtain  $E[T_{go} | T_{go} < T_{stop} + t_d] = 1/(\lambda_{go} + \lambda_{stop})$ , consistent with the density we mentioned above 754  
 682 for this value of the stop signal delay. 755

745 **PND model: exponential example.** Inserting exponential margins into the bivariate distribution,

$$\begin{aligned}
 H^-(s, t) &= \max\{F_{go}(s) + F_{stop}(t) - 1, 0\} \\
 &= \max\{1 - \exp[-\lambda_{go} s] - \exp[-\lambda_{stop} t], 0\},
 \end{aligned}
 \tag{21}$$

749 for all  $s, t \geq 0$ . From [14],

$$\begin{aligned}
 p_r(t_d) &= \Pr[T_{go} - T_{stop} < t_d] \\
 &= \Pr[T_{go} - F_{stop}^{-1}[1 - F_{go}(T_{go})] < t_d] \\
 &= \Pr[T_{go} - F_{stop}^{-1}[\exp(-\lambda_{go} T_{go})] < t_d] \\
 &= \Pr[T_{go} + 1/\lambda_{stop} \log[1 - \exp(-\lambda_{go} T_{go})] < t_d] \\
 &= \Pr[g(T_{go}) < t_d] \\
 &= \Pr[T_{go} < g^{-1}(t_d)].
 \end{aligned}
 \tag{22}$$

759 Note that function

$$g(T_{go}) \equiv T_{go} + 1/\lambda_{stop} \log[1 - \exp(-\lambda_{go} T_{go})]$$

762 cannot be solved explicitly for  $T_{go}$ . Therefore, in order to compute  $p_r(t_d)$  and plot signal-response time distributions

$$F_{sr}(t | t_d) = F_{go}(\min\{t, g^{-1}(t_d)\})/F_{go}(g^{-1}(t_d)),$$

765 we sampled ( $n = 100,000$ ) from the bivariate distribution function  $H^-(s, t)$  using function **simCop** (based on the conditional simulation method, see (22)) from the **copBasic** package of the open source software R (<http://www.r-project.org>).

767 Table 1 lists the crossing points for the signal-response time distributions obtained from the simulation. They correspond to the vertical lines in Figure 1.

**Table 1. Predictions for crossing points  $F_{sr}(t | t_d) = 1.0$  in PND model**

$t_d$ [ms]	10	50	100	150
$g^{-1}(t_d)$	53.6	79.9	117.7	161.4

Compare with Figure 1

## 778 Supporting Information (SI)

780 **Fréchet-Hoeffding bounds and perfect dependency.** The dependence between two random variables of a random vector  $(X, Y)$  is completely described by its probability distribution. Let  $G(x, y)$  be the bivariate distribution function of some random vector  $(X, Y)$ :

$$G(x, y) = P(X \leq x, Y \leq y)$$

784 with marginal distributions  $F_X$  and  $F_Y$ . Then, it always holds that

$$\begin{aligned}
 G^-(x, y) &= \max\{F_X(x) + F_Y(y) - 1, 0\} \leq G(x, y) \\
 &\leq \min\{F_X(x), F_Y(y)\} = G^+(x, y),
 \end{aligned}$$

789 for all  $x, y$  for which  $G$  is defined (the support of  $G$ ). Both  $G^-(x, y)$  and  $G^+(x, y)$  are known as *Fréchet-Hoeffding bounds* and are themselves distribution functions for  $(X, Y)$ :  $G^-$  corresponds to “perfect” negative dependence between  $X$  and  $Y$ , while  $G^+$  corresponds to “perfect” positive dependence (see (22) for proofs of this and other claims in this section). “Perfect” dependency can be formulated in various ways. For simplicity, we assume  $X$  and  $Y$  have continuous distribution functions, the only case we will need below. Here are three equivalent characterizations of *perfect negative dependence* (analogous results exist for perfect positive dependence, but they are not of concern here):

795 (i) Either  $\Pr(X > x, Y > y) = 0$  for all  $x, y$  or

$$\Pr(X \leq x, Y \leq y) = 0 \text{ for all } x, y;$$

798 (ii)  $\Pr[F_X(X) + F_Y(Y) = 1] = 1$ ;

800 (iii)  $X$  is almost surely a decreasing function of  $Y$ .

801 Consider the equation inside the “Pr” expression in (ii): Solving for  $X$  by taking the inverse function of  $F_X(X)$  we get

$$X = F_X^{-1}[1 - F_Y(Y)],$$

805 from which (iii) follows. Random variables with perfect negative dependence are also known as *antithetic variates* in simulation studies.

869	1. D. Algom, A. Eidels, R.X.D. Hawkins, B. Jefferson, and J.T. Townsend. Features of response times: identification of cognitive mechanisms through mathematical modeling. In J.R. Busemeyer, Z. Wang, J.T. Townsend, and A. Eidels, editors, <i>The Oxford Handbook of Mathematical and Computational Psychology</i> , chapter 4, pages 63–98. Oxford University Press, New York, NY 10016, 2015. ISBN 9780199957996.	931
870		932
871	2. J.T. Townsend. Serial vs. parallel processing: Sometimes they look like tweedledum and tweedledee but they can (and should be) distinguished. <i>Psychological Science</i> , 1:46–54, 1990.	933
872	3. J.T. Townsend and M.J. Wenger. A theory of interactive parallel processing: new capacity measures and predictions for a response time inequality series. <i>Psychological Review</i> , 111(4):1003–1035, 2004.	934
873	4. B.U. Forstmann and E.J. Wagenmakers, editors. <i>An introduction to model-based cognitive neuroscience</i> . Springer-Verlag GmbH, New York Heidelberg Dordrecht London, 1st edition, 2015. ISBN 978-1-4939-2235-2. URL <a href="http://www.ebook.de/de/product/22860990/an_introduction_to_model_based_cognitive_neuroscience.html">http://www.ebook.de/de/product/22860990/an_introduction_to_model_based_cognitive_neuroscience.html</a> .	936
874	5. G.D. Logan. Takong control of cognition: an instance perspective on acts of control. <i>American Psychologist</i> , 72(9):875–884, 2017.	937
875	6. F. Verbruggen and G.D. Logan. Models of response inhibition in the stop-signal and stop-change paradigms. <i>Neuroscience &amp; Biobehavioral Reviews</i> , 33:647–661, 2009. <a href="http://doi.org/10.1016/j.neubiorev.2008.08.014">http://doi.org/10.1016/j.neubiorev.2008.08.014</a> .	938
876	7. G.D. Logan. On the ability to inhibit thought and action: A users' guide to the stop signal paradigm. In D. Dagenbach and T.H. Carr, editors, <i>Inhibitory processes in attention, memory, and language</i> , pages 189–239. Academic Press, San Diego, 1994.	939
877		940
878	8. F. Verbruggen and G.D. Logan. Response inhibition in the stop-signal paradigm. <i>Trends in Cognitive Sciences</i> , 12:418–424, 2008. <a href="http://doi.org/10.1016/j.tics.2008.07.005">http://doi.org/10.1016/j.tics.2008.07.005</a> .	941
879	9. D. Matzke, F. Verbruggen, and G.D. Logan. The stop-signal paradigm. In E.J. Wagenmakers, editor, <i>Stevens' Handbook of Experimental Psychology and Cognitive Neuroscience: Methodology</i> , volume 4. John Wiley & Sons, 4th edition, in press.	942
880		943
881	10. R. Carpenter and I. Noorani. Preface: Movement suppression: brain mechanisms for stopping and stillness. volume 372 of <i>Philosophical Transactions of the Royal Society B</i> . The Royal Society Publishing, 2017. 10.1098/rstb.2016.0542.	944
882	11. G.D. Logan and W.B. Cowan. On the ability to inhibit thought and action: a theory of an act of control. <i>Psychological Review</i> , 91(3):295–327, 1984.	945
883	12. J.D. Schall, T.J. Palmeri, and G.D. Logan. Models of inhibitory control. <i>Philosophical Transactions of the Royal Society of London B</i> , 372(20160193), 2017. <a href="http://dx.doi.org/10.1098/rstb.2016.0193">http://dx.doi.org/10.1098/rstb.2016.0193</a> .	946
884	13. D.P. Hanes and J.D. Schall. Countermanding saccades in macaque. <i>Visual Neuroscience</i> , 12:929–937, 1995.	947
885	14. D.P. Hanes, W.F. Patterson, and J.D. Schall. Role of frontal eye field in countermanding saccades: visual, movement and fixation activity. <i>Journal of Neurophysiology</i> , 79:817–834, 1998.	948
886	15. M. Paré and D.P. Hanes. Controlled movement processing: superior colliculus activity associated with countermanded saccades. <i>Journal of Neuroscience</i> , 23:6480–6489, 2003.	949
887	16. J.W. Brown, D.P. Hanes, J.D. Schall, and V. Stuphorn. Relation of frontal eye field activity to saccade initiation during a countermanding task. <i>Experimental Brain Research</i> , 190:135–151, 2008. DOI 10.1007/s00221-008-1455-0.	950
888	17. L. Boucher, T.J. Palmeri, G.D. Logan, and J.D. Schall. Inhibitory control in mind and brain: an interactive race model of countermanding saccades. <i>Psychological Review</i> , 114(2):376–397, 2007.	951
889	18. J.D. Schall and D.C. Godlove. Current advances and pressing problems in studies of stopping. <i>Current Opinion in Neurobiology</i> , 22:1012–1021, 2012.	952
890	19. D.P. Hanes and J.D. Schall. Neural control of voluntary movement initiation. <i>Science</i> , 274:427–430, 1996.	953
891	20. G.D. Logan, M. Yamaguchi, J.D. Schall, and T.J. Palmeri. Inhibitory control in mind and brain 2.0: Blocked-input models of saccadic countermanding on the ability to inhibit thought and action: General and special theories of an act of control. <i>Psychological Review</i> , 122:115–147, 2015.	954
892	21. C.C. Lo, L. Boucher, M. Paré, J.D. Schall, and X.J. Wang. Proactive inhibitory control and attractor dynamics in countermanding action: a spiking neural circuit model. <i>Journal of Neuroscience</i> , 29:9059–9071, 2009.	955
893	22. R. B. Nelsen. <i>An introduction to copulas</i> , volume 139 of <i>Lecture Notes in Statistics</i> . Springer-Verlag, New York, NY, 2nd edition, 2006.	956
894	23. M. Denuit and J. Dhaene. Simple characterizations of comonotonicity and countermonotonicity by extremal correlations. <i>Belgian Actuarial Bulletin</i> , 3(1):22–27, 2003.	957
895	24. P.G. Bissett and G.D. Logan. Selective stopping? Maybe not. <i>Journal of Experimental Psychology: General</i> , 143(1):455–472, 2014.	958
896	25. H. Colonius. A note on the stop-signal paradigm, or how to observe the unobservable. <i>Psychological Review</i> , 97(2):309–312, 1990.	959
897	26. G.P.H. Band, M.W. van der Molen, and G.D. Logan. Horse-race model simulations of the stop-signal procedure. <i>Acta Psychologica</i> , 112:105–142, 2003.	960
898	27. D. Matzke, C.V. Dolan, G.D. Logan, S.D. Brown, and E.-J. Wagenmakers. Bayesian parametric estimation of stop-signal reaction time distributions. <i>Journal of Experimental Psychology: General</i> , 142(4):1047–1073, 2013.	961
899		962
900	<b>Figure caption for Figure 1.</b> The “fan” effect: all signal-response RT distributions $F_{sr}(t t_d)$ are strictly ordered by delay ( $t_d$ ) from left to right, for $t_d = 10, 50, 100, 150$ [ms], converging toward no-stop signal distribution $F_{go}(t)$ (rightmost curve) for $t_d \rightarrow \infty$ , for exponential distributions with rate parameters $\lambda_{go} = .01$ and $\lambda_{stop} = .02$ ; PND model curves were obtained by simulation (see Methods); dashed: IND model; solid: PND model.	963
901		964
902		965
903		966
904		967
905		968
906		969
907		970
908		971
909		972
910		973
911		974
912		975
913		976
914		977
915		978
916		979
917		980
918		981
919		982
920		983
921		984
922		985
923		986
924		987
925		988
926		989
927		990
928		991
929		992
930		



993  
994  
995  
996  
997  
998  
999  
1000  
1001  
1002  
1003  
1004  
1005  
1006  
1007  
1008  
1009  
1010  
1011  
1012  
1013  
1014  
1015  
1016  
1017  
1018  
1019  
1020  
1021  
1022  
1023  
1024  
1025  
1026  
1027  
1028  
1029  
1030  
1031  
1032  
1033  
1034  
1035  
1036  
1037  
1038  
1039  
1040  
1041  
1042  
1043  
1044  
1045  
1046  
1047  
1048  
1049  
1050  
1051  
1052  
1053  
1054

1055  
1056  
1057  
1058  
1059  
1060  
1061  
1062  
1063  
1064  
1065  
1066  
1067  
1068  
1069  
1070  
1071  
1072  
1073  
1074  
1075  
1076  
1077  
1078  
1079  
1080  
1081  
1082  
1083  
1084  
1085  
1086  
1087  
1088  
1089  
1090  
1091  
1092  
1093  
1094  
1095  
1096  
1097  
1098  
1099  
1100  
1101  
1102  
1103  
1104  
1105  
1106  
1107  
1108  
1109  
1110  
1111  
1112  
1113  
1114  
1115  
1116

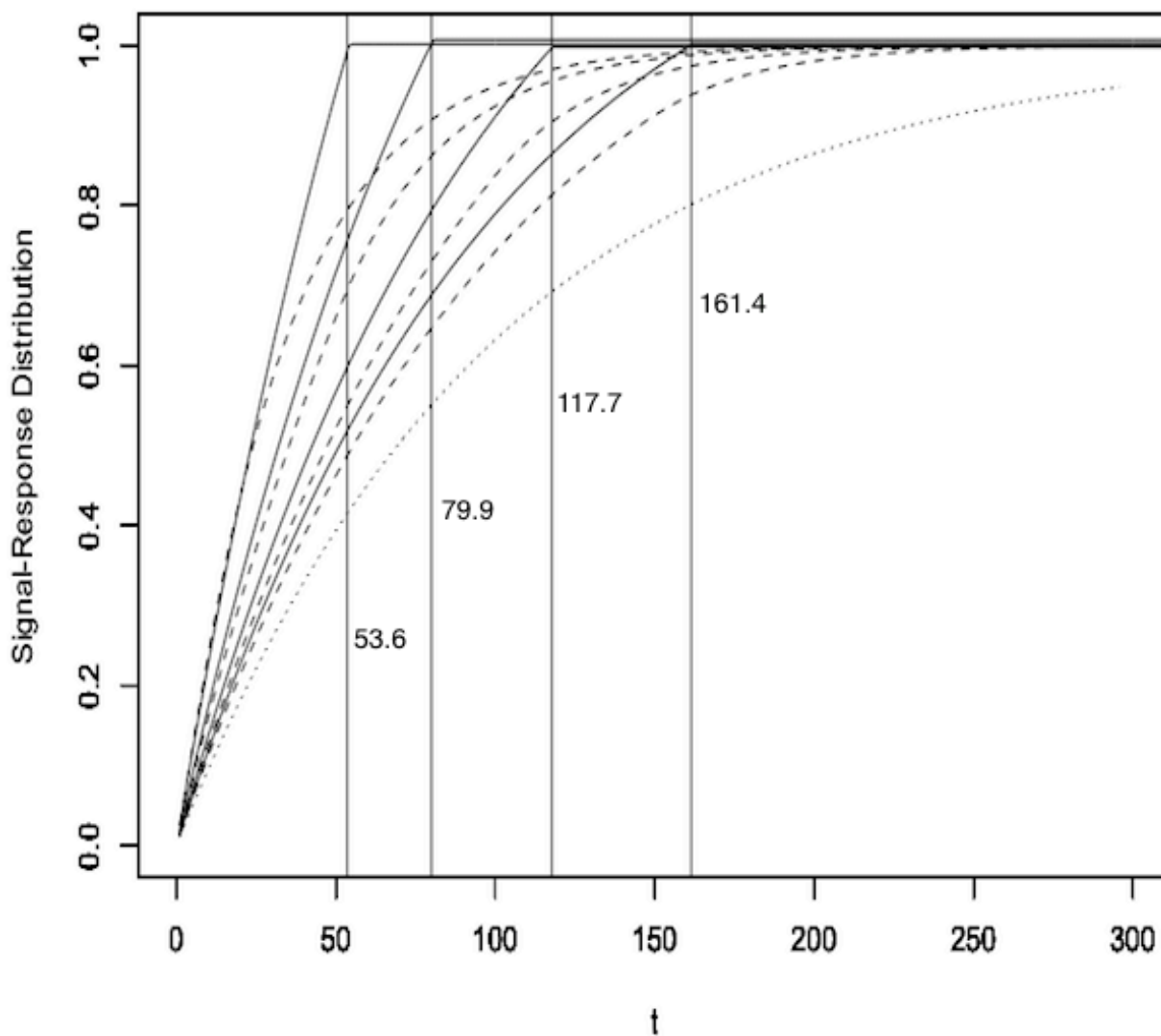


Fig. 1